arXiv:2505.03201v1 [stat.ML] 6 May 2025

Weighted Average Gradients for Feature Attribution

Tran Duc Tuan Kien[1], Nguyen Trong Tam[1], Nguyen Hoang Son[1], Than Quang Khoat[1], Nguyen Duc Anh[1*]

[1]School of Information Technology and Communication, Hanoi University of Science and Technology, Dai Co Viet, Hanoi, 10000, Hanoi, Vietnam.

*Corresponding author(s). E-mail(s): anhnd@soict.hust.edu.vn; Contributing authors: keinnaut@gmail.com; nguyentrongtam2409@gmail.com; hoangson13022004@gmail.com,; khoattq@soict.hust.edu.vn;

Abstract

In explainable AI, Integrated Gradients (IG) is a widely adopted technique for assessing the significance of feature attributes of the input on model outputs by evaluating contributions from a baseline input to the current input. The choice of the baseline input significantly influences the resulting explanation. While the traditional Expected Gradients (EG) method assumes baselines can be uniformly sampled and averaged with equal weights, this study argues that baselines should not be treated equivalently. We introduce Weighted Average Gradients (WG), a novel approach that unsupervisedly evaluates baseline suitability and incorporates a strategy for selecting effective baselines. Theoretical analysis demonstrates that WG satisfies essential explanation method criteria and offers greater stability than prior approaches. Experimental results further confirm that WG outperforms EG across diverse scenarios, achieving an improvement of 10-35% on main metrics. Moreover, by evaluating baselines, our method can filter a subset of effective baselines for each input to calculate explanations, maintaining high accuracy while reducing computational cost. The code is available at: https://github.com/Tamnt240904/weighted_baseline.

Keywords: explainable AI, feature attribution, integrated gradients, expected gradients

1 Introduction

Explainable AI (XAI) is becoming increasingly vital as machine learning and deep learning models achieve high performance across various applications. As these models are integrated into critical decision-making processes, understanding their behavior and ensuring transparency is essential for building trust and accountability. Among these domains, feature attribution has become a significant area of research. This subfield focuses on determining the contribution and influence of individual input features on output predictions. Feature attribution is typically achieved by assigning importance scores to each feature, which helps to decipher the decision-making process of the model.

The exploration of feature attribution methods has a long history, but it gained significant traction with the introduction of Integrated Gradients ([1]). Drawing inspiration from path-based approaches ([2]), IG measures the contribution of each feature by integrating gradients along a path from a carefully chosen baseline to the current input. This technique is deeply rooted in theoretical foundations, notably the principles of Shapley values from cooperative game theory ([3]), which provide a robust framework for fairly distributing credit among features. By tracing this interpolated path, IG offers a principled way to attribute model outputs, making it a cornerstone in the quest for interpretable AI.

While Integrated Gradients and its variants satisfy several meaningful axioms, they are not without their shortcomings. [4] has identified three main issues associated with path methods: baseline selection, path selection, and counterintuitive scores. Among these, baseline selection remains a significant challenge due to the inherent differences between baselines in the context of AI and Economy, which is the absence of a truly neutral baseline in AI contexts. This leads to inconsistencies in results across different baselines. No single baseline proves effective across all inputs, and the theoretical interplay between baseline choice and the outcomes of path-based methods remains underexplored.

To mitigate these inconsistencies, the Expected Gradient ([5]) method takes averaging results over multiple baselines. This approach helps reduce the impact of poorly chosen baselines; however, it operates under the assumption that all baselines hold equal significance within the baseline space. This assumption is overly simplistic and impractical since each baseline can have varying degrees of relevance or "fitness" concerning specific inputs. Consequently, if a substantial number of baselines are suboptimal, they can skew the final results significantly since both worse and good baselines have same effect

In this paper, we propose a novel approach that meticulously evaluates the fitness of each baseline and approximates a more accurate distribution of baseline for aggregation. We argue that the fitness—or quality—of a baseline is inherently tied to both the input and the baseline itself, meaning changes in either can shift its suitability. Baselines with higher fitness are more likely to produce faithful explanations and should thus exert greater influence in the final attribution, while less suitable baselines should contribute less. Unlike Expected Gradients, which treats all baselines

uniformly without regard for their individual characteristics or input-specific relevance, our method leverages fitness scores to construct a distribution where baselines offering more reliable explanations are prioritized.

To formalize this idea, we introduce an unsupervised fitness function that assesses baseline quality based on the input and reference points, eliminating the need for subjective human judgment. We complement this with an efficient algorithm to compute baseline fitness, achieving a time complexity of $O(\log n)$. These fitness scores are then used to interpolate weights, which guide the aggregation of intermediate results from each baseline. Through rigorous experimentation, we benchmark our proposed method against existing techniques, showcasing its superior accuracy and reliability in generating explanations. Furthermore, we provide a theoretical analysis demonstrating that our approach preserves the critical axioms and intuitions of path-based methods while delivering greater stability than Expected Gradients—a testament to its enhanced precision.

Beyond improving explanation quality, our method yields an additional practical advantage: by assessing baseline fitness, we can filter out suboptimal baselines, streamlining computation without sacrificing the accuracy of the final explanation. This dual benefit of heightened efficiency and maintained fidelity sets our approach apart.

In summary, our research tackles longstanding challenges in feature attribution methods like Integrated Gradients by refining baseline selection and weighting through a sophisticated fitness measure. This advancement not only elevates the precision and effectiveness of AI-generated explanations but also represents a significant step forward in the broader field of explainable AI.

2 Related Works

Explainable AI can be categorized into perturbation-based, backpropagation-based, and attention-based approaches. Perturbation-based techniques ([6], [7], [8]) assess feature importance by systematically altering inputs or neurons and observing their effects on model predictions. While intuitive, these methods demand repeated forward passes through the network, rendering them computationally expensive and impractical for real-time applications or integration into training pipelines. In contrast, backpropagation-based methods ([9], [10],[11],[12]) leverage gradients or predefined rules to propagate importance signals from outputs to inputs. These approaches are notably efficient, scalable to high-dimensional data, and readily implemented on GPUs, making them ideal for differentiable models without requiring architectural modifications. Meanwhile, attention-based methods ([13],[14],[15]), prevalent in transformer architectures, exploit attention weights to pinpoint influential input regions, where higher weights signify greater relevance to predictions. Each paradigm offers unique strengths, yet backpropagation-based methods—particularly gradient-based variants—stand out for their balance of efficiency and interpretability, forming the foundation of our investigation.

Integrated Gradients [1] has emerged as a foundational technique in XAI. By integrating gradients along a path from a baseline to the input, IG assigns pixel-level attribution scores that reflect each feature's contribution to the model's output.

Rooted in axiomatic principles like completeness and sensitivity, and inspired by cooperative game theory's Shapley values ([3]), IG provides a theoretically sound framework for interpretability. However, its effectiveness hinges on critical design choices, as highlighted by Naveed Akhtar ([4]: baseline selection, path selection, and the risk of counterintuitive scores. Of these, baseline selection remains a persistent challenge, as the absence of a universally neutral baseline in AI—unlike in economic contexts—introduces variability that can compromise explanation quality.

To address IG's sensitivity to baselines, prior works have explored diverse strategies. Some approaches learn optimal baselines from data, seeking reference points that represent a neutral or "uninformative" state for the model ([16]). Expected Gradients ([5]) takes a different tack, sampling multiple baselines and averaging their attributions to mitigate the impact of any single suboptimal choice. While effective in reducing noise, EG assumes uniform significance across baselines—an oversimplification that overlooks their varying relevance to specific inputs. Shapley Integrated Gradients (SIG) ([17]) refines this by constructing baselines via proportional sampling, aligning with game-theoretic Shapley value computations to enhance fairness in attribution. Meanwhile, path selection innovations like Guided Integrated Gradients ([18]) adaptively choose integration paths by prioritizing features with minimal partial derivatives, and Blur IG ([16]) integrates gradients along a progressively blurred image trajectory, tailoring the explanation to perceptual shifts.

Beyond path-based methods, the concept of weighting components within attribution frameworks has gained traction elsewhere. Weighted-SHAP ([19]), for instance, adjusts Shapley values with weights reflecting feature dependencies, yielding more accurate and interpretable scores. Similarly, Integrated Decision Gradients (IDG) ([20]) nad IDIG ([21]) assign weights to interpolation points along the IG path, emphasizing regions where the model's logits shift most dramatically. These efforts underscore the potential of weighted aggregation to capture nuanced relationships in data and model behavior, yet their application to baseline selection in IG remains underexplored.

Our work bridges this gap by introducing Weighted Average Gradients (WG), a pioneering approach that evaluates baseline fitness in an unsupervised manner to approximate an optimal baseline distribution. Unlike EG's equal-weight averaging or SIG's game-theoretic sampling, WG assigns weights to baselines based on their input-specific suitability, ensuring that more faithful baselines exert greater influence. This fitness-driven weighting not only enhances explanation accuracy—outperforming EG by 24.8% on key metrics, as shown in our experiments—but also enables efficient computation by filtering out suboptimal baselines. By marrying theoretical stability with practical efficiency, WG advances the state of the art in feature attribution, offering a robust, scalable solution for interpretable AI that aligns with the demands of modern deep learning applications.

3 Background

In this section, we brief key concepts of Integrated Gradients, Expected Gradients and then highlight the limitations of Expected Gradients. Reformulating Integrated

Gradients as a gradient path integral and Expected Gradients as a uniform baseline expectation reveals Expected Gradients's key flaw: its oversimplified assumption that all baselines contribute equally, disregarding their relevance to specific inputs. This limitation motivates our proposed method, detailed next, which refines baseline weighting for more accurate and stable explanations.

3.1 Intergrated Gradient

Integrated Gradients addresses the saturation problem by aggregating gradients along a path from a reference point or baseline x' to the input x. Inspired by game-theoretic principles, IG starts at a reference point—ideally a neutral state where the input offers minimal information—and traces a trajectory where features incrementally shape the model's prediction.

Formally, given a classifier, a class c, and an input x, the output $f_c(x)$ represents the probability of predicting x as belonging to class c. The Integrated Gradients calculate the attribution for the ith feature as:

$$\text{IntegratedGradients}_i(x, x') := (x_i - x'_i) \times \int_0^1 \frac{\partial f(x' + \alpha(x - x'))}{\partial x_i} \, d\alpha, \tag{1}$$

where $\frac{F(x)}{x_i}$ is the gradient of F along the ith feature and α parameterizes the interpolated coefficient of points that lie between input and the reference point x' ($\alpha \in [0, 1]$). This integral captures each feature's contribution by averaging its gradient's influence across the path.

A pivotal challenge in path-based methods like IG lies in selecting an effective baseline. The path from x' to x dictates feature importance: if x' preserves key feature values from x, the difference $x_i - x'_i$ shrinks, and the integral assigns near-zero importance, potentially masking critical contributions. Conventionally, a "neutral" baseline—often a zero vector—is chosen, presumed to lack informational content. Yet, in deep learning, neutrality is elusive; models like object detectors assign non-trivial predictions even to zeroed (black) images, distributing probabilities across classes with a sum of one. This reveals a stark reality: a zero vector, or any fixed baseline, may not universally serve as an uninformative reference.

Empirical evidence underscores that baseline choice profoundly impacts explanation quality, yet no rigorous theory defines an optimal x' for arbitrary inputs. A baseline effective for one image may falter for another, necessitating laborious, image-specific tuning that remains suboptimal and impractical. This variability exposes a gap in path-based XAI: the lack of a principled, adaptive strategy for baseline selection.

3.2 Expected Gradient and Oversimplification

a. Reformulation of Expected Gradients

To confront the baseline selection challenge in Integrated Gradients (IG), several variants have emerged, with Expected Gradients (EG) [5] standing as a prominent and widely adopted solution. Instead of using a single baseline, EG approximates integrated gradients over multiple baselines. Each reference point has different characteristics; thus, when computing IG, this method aims for each baseline to highlight

different important points. EG ensembles explanations from these baselines to create a final explanation, with the hope that the model can cover all important points, and averaging the explanations leads to a more stable result.

$$\text{ExpectedGradients}_i(x) := \int_{x'} \text{IntegratedGradients}_i(x, x') p_D(x')\, dx', \tag{2}$$

More specifically, EG assumes a distribution of baselines, which is a space of images. The novel explanation is then the expected value of integrated gradients over all baselines, which can be assumed to reflect all important points of the image.

Since each baseline has different characteristics, they will provide different levels of faithfulness to the optimal explanation. We define this as fitness. A baseline with high fitness will produce good explanations. Therefore, in the distribution of baselines, we want baselines with high fitness to have a greater impact on the expectation; that is, they should have a higher probability when computing the expectation. In other words, we want the density function to be proportional to fitness.

$$\text{ExpectedGradients}_i(x) \approx \sum_{x' \in D'} \text{IntegratedGradients}_i(x, x') p_D(x') dx' \tag{3}$$

$$\approx \sum_{x' \in D'} (x_i - x'_i) \times \frac{\delta f(x' + \alpha \times (x - x'))}{\delta x_i}. \tag{4}$$

Since the space of all possible baselines is infinitely large, EG handles this issue using a sampling method. Baselines are drawn uniformly, interpolation points are traced along their paths, and their gradients are averaged to approximate the expectation. This approach, while pragmatic, harbors a critical flaw: uniform sampling implicitly assigns equal probability—or fitness—to every baseline, flattening their contributions into a democratic but misguided chorus.

b. Oversimplicification of Expected Gradients

In Equation (1), Integrated Gradients calculate the attribution of characteristics by integrating the gradients of the model output with respect to the input features along a path from a baseline x' to the actual input x, parameterized by an interpolation factor $\alpha \in [0, 1]$. The ideal explanation for an input would emerge as the true expected value of these integrated gradients over a distribution of baselines. However, the infinite expanse of possible baselines renders this expectation computationally intractable, prompting Expected Gradients to approximate it via sampling. Specifically, EG estimates this expectation as:

$$\hat{EG}(x) = \frac{1}{n} \sum_{i=1}^{n} \left((x_i - x'_i) \times \frac{\partial f(x' + \alpha(x'_i) \cdot (x - x'_i))}{\partial x_i} \right), \tag{5}$$

Central to EG's methodology is the assumption that all baselines x_k' are equally significant, as they are drawn from a uniform distribution and contribute symmetrically to the averaged gradient. This uniform weighting implies that each baseline carries identical informational value, irrespective of its relevance to the input or the model's behavior.

This assumption, however, is compromised and overly reductive. Baselines exhibit a spectrum of informativeness—some align closely with the model's decision manifold, yielding gradients that faithfully reflect feature importance, while others deviate, producing noisy or misleading signals. By enforcing a uniform distribution, EG disregards this heterogeneity, equating the influence of high-fidelity baselines with those of lesser utility. Such an egalitarian approach risks diluting the signal from informative reference points, skewing the final attribution away from the model's true reasoning. Theoretical scrutiny reveals that this oversimplification misaligns EG's approximation with the ideal expectation, undermining its reliability as a faithful interpretative tool.

To rectify this, a more principled approximation must transcend uniformity and embrace a distribution that mirrors the baselines' differential contributions. We contend that the baseline distribution should be weighted by a notion of fitness—a metric capturing each baseline's capacity to generate accurate and meaningful gradients for a given input. By prioritizing baselines with higher fitness, the aggregation can amplify the signal of those most aligned with the model's decision process, yielding an explanation that more precisely approximates the true expected gradient. This fitness-driven paradigm not only addresses EG's shortcomings but also elevates the interpretability of gradient-based methods, a direction we explore rigorously with our Weighted Average Gradients (WG) framework.

4 Proposed Method

In this section, we propose Weighted Average Gradients (WG), a novel advancement that redefines baseline selection in Integrated Gradients (IG) through a perturbation-based fitness measure. WG departs from the limitations of prior methods by assigning weights to baselines according to their explanatory fidelity, thereby enhancing the precision and robustness of feature attributions.

$$\mathrm{WG}_i(x) = \sum_{k=1}^{n} w_k \cdot \left[(x_i - x_{k,i}) \cdot \int_0^1 \frac{\partial f(x'_k + \alpha \cdot (x - x_k))}{\partial x_i} d\alpha \right] \tag{6}$$

where w_k represents the weight of the (k)-th baseline x'_k, derived from its fitness, and the integral computes the IG attribution for each baseline. By modulating the influence of each baseline via w_k, WG ensures that more informative reference points dominate the aggregation, yielding a final explanation that better reflects the model's decision-making process.

4.1 Fitness Measure Based on Perturbation

Perturbation stands as one of the most natural approaches for assessing the roles of individual elements within a complex set. In the context of explainable AI, especially concerning baseline selection in Integrated Gradients, perturbation offers an intuitive way to evaluate the impact of each baseline on the resulting explanation. By systematically altering or removing features and observing the corresponding changes in the model's output, we can effectively gauge the significance of each baseline in highlighting critical aspects of the input.

Crucially, perturbation-based methods eliminate the need for manual annotations, harnessing the model itself to evaluate output perturbations. This renders the method both efficient and objective, purging the subjectivity that often plagues human-driven assessments.

We, therefore, propose a fitness function to measure the quality of a baseline with respect to each input. The fitness function, denoted as D_α, is defined as the minimum number of features that need to be removed to reduce the model's predicted output score to $\alpha\%$ of its original value. Mathematically, we define D_α as:

$$D_\alpha = \min\{|S| : S \subseteq F, f(x \circ M(S)) \leq \alpha \cdot f(x)\} \tag{7}$$

D_α represents the minimal number of features in subset S (drawn from the full feature set F) that, when masked via $M(S)$ (setting them to zero or a neutral value), reduces the model's output score $f(x)$ to $\alpha\%$ of its original value. Here, $x \circ M(S)$ denotes the element-wise product of the input x with the mask $M(S)$, and $\alpha \in (0, 1)$ is a predefined threshold. For each baseline x'_k, we compute its IG attribution, yielding a temporary explanation that highlights distinct regions of importance. The fitness D_α then evaluates this explanation: a smaller D_α indicates that masking fewer features—those deemed critical by the baseline—precipitates a sharp drop in $f(x)$, signaling high fidelity in pinpointing influential features.

This metric is both principled and pragmatic. A baseline with a low D_α aligns tightly with the model's sensitivity, amplifying features that drive predictions, while a high D_α suggests a disconnect, diluting focus on extraneous elements. When aggregating these intermediate attributions in WG, we assign weights:

$$w_k \propto \frac{1}{D_\alpha} \tag{8}$$

, ensuring that baselines with greater fitness exert stronger influence. This weighting mirrors a probabilistic intuition: baselines with high explanatory power should dominate the expectation, akin to a density function skewed toward fidelity. The elegance of D_α lies in its unsupervised nature and input-baseline synergy.

4.2 Algorithm for Efficient Fitness Calculation

To compute D_α, the minimal number of features to mask to reduce the model's output score to $\alpha\%$ of its original value, a naive exhaustive search would incur a prohibitive $O(n)$ time complexity, where n is the number of features. Leveraging the monotonicity of score reduction upon feature removal, we propose an efficient binary search strategy, achieving a time complexity of $O(\log n)$ per baseline. The algorithm iteratively adjusts the proportion of features masked—guided by their importance scores (e.g., IG attributions)—until the target score is approximated within a tolerance ϵ.

Algorithm 1 Compute_D_alpha

Require: x: input data (e.g., image)
Require: $attr$: feature importance scores (e.g., IG attributions)
Require: f: model function (classifier)
Require: α: target score reduction ratio ($0 < \alpha < 1$)
Require: $neutral$: neutral value for masked features
Require: ε: convergence threshold
Ensure: d_α: minimal number of removal pixels

```
target_score ← α · f(x)
low ← 0
high ← count(x)
while low ≤ high do
    mid ← ⌊(low + high)/2⌋
    mask ← FindMask(attr, mid)
    x' ← x · (1 − mask) + neutral · mask
    if |f(x') − target_score| < ε then
        return mid
    else if f(x') < target_score then
        low ← mid + 1
    else
        high ← mid − 1
    end if
end while
return mid
```

5 Theoretical Analysis

In this section, we formally analyze the axiomatic properties satisfied by our proposed Weighted Average Gradients (WG) method, a principled extension of Expected Gradients (EG) that aggregates multiple baseline explanations using fitness-weighted averaging. We examine three core desiderata of attribution methods: *completeness*, *sensitivity*, and *implementation invariance*. Furthermore, we show that WG is more stable than EG with variance reduction property. For the proofs of these properties, please refer to Appendix B.

5.1 Completeness

Completeness ensures that the sum of attributions over all input features equals the difference between the model output at the input and the expected output over the baselines. WG inherits and generalizes this property from IG by computing fitness-weighted attributions across baselines.

Theorem 1 (Completness of WG) *Let f be the model, x the input, and $\{x'_k\}_{k=1}^n$ a set of baselines with associated normalized weights w_k (i.e., $\sum_{k=1}^n w_k = 1$). With WG attribution for feature i:*

$$\phi_i^{WG}(x) = \sum_{k=1}^{n} w_k \cdot \phi_i^{IG}(x, x'_k)$$

then:

$$\sum_{i=1}^{d} \phi_i^{WG}(x) = f(x) - \sum_{k=1}^{n} w_k f(x'_k) = f(x) - \mathbb{E}_{x' \sim p_w}[f(x')]$$

The preservation of completeness in WG is not merely a formality—it underscores the method's fidelity to the model's behavior. By weighting baselines according to their fitness, WG ensures that the aggregated explanation remains consistent with the total change in model output, while prioritizing baselines that better capture the model's decision-making process. This balance of theoretical rigor and practical enhancement positions WG as a robust advancement in gradient-based explainability, aligning with the axiomatic foundations expected in high-impact XAI research.

5.2 Sensitivity

The *sensitivity axiom* is a cornerstone of feature attribution methods, ensuring that attributions accurately reflect the influence of input features on model predictions. It comprises two conditions: Sensitivity(a), which mandates non-zero attributions for features that impact the model's output, and Sensitivity(b), which requires zero attributions for features with no influence. In this section, we rigorously prove that Weighted Average Gradients (WG) satisfies both conditions, leveraging its fitness-weighted aggregation of Integrated Gradients (IG) paths to maintain theoretical fidelity while enhancing explanatory precision.

Consider a differentiable model $f : \mathbb{R}^d \to \mathbb{R}$, an input $x \in \mathbb{R}^d$, and a set of baselines $\{x'_k\}_{k=1}^n$. The WG attribution for feature (i) is defined as:

$$\phi_i^{\mathrm{WG}}(x) = \sum_{k=1}^{n} w_k \cdot \phi_i^{\mathrm{IG}}(x, x'_k)$$

where

$$\phi_i^{\mathrm{IG}}(x, x'_k) = (x_i - x'_{k,i}) \int_0^1 \frac{\partial f(x'_k + \alpha(x - x'_k))}{\partial x_i} d\alpha$$

is the IG attribution for baseline x'_k, and $w_k \geq 0$ are fitness-derived weights satisfying $\sum_{k=1}^{n} w_k = 1$. We now establish that WG adheres to both Sensitivity(a) and Sensitivity(b).

Theorem 2 (Sensitivity of WG) ***a) Non-Zero Attribution for Influential Features***
If feature $x_i \neq x'_{k,i}$ for some baseline x'_k, and x_i affects $f(x)$ (i.e., $\frac{\partial f}{\partial x_i} \neq 0$ along the path), then:

$$\phi_i^{WG}(x) \neq 0$$

b) Zero Attribution for Non-Influential Features

Sensitivity(b) requires that if feature x_i has no impact on $f(x)$, i.e., $\frac{\partial f}{\partial x_i} = 0$ everywhere, then:

$$\phi_i^{WG}(x) = 0$$

The satisfaction of both Sensitivity(a) and Sensitivity(b) underscores WG's alignment with the axiomatic principles of explainable AI. By inheriting IG's sensitivity properties and enhancing them through fitness-weighted aggregation, WG ensures that attributions are both meaningful and precise—non-zero only for features that genuinely affect the model, and zero otherwise. This dual compliance not only validates WG's theoretical soundness but also amplifies its practical utility, making it a compelling advancement for gradient-based interpretability in complex models.

5.3 Implementation Invariance

The **implementation invariance axiom** is a critical requirement for feature attribution methods, ensuring that models with identical input-output mappings—despite differing architectures—yield identical attributions. This property guarantees that explanations are tied solely to the model's functional behavior, not its internal structure, fostering consistency across diverse implementations. In this section, we demonstrate that Weighted Average Gradients (WG) rigorously satisfies this axiom, leveraging its gradient-based foundation and fitness-weighted aggregation to maintain invariance while enhancing explanatory fidelity.

Theorem 3 (Implementation Invariance) *Consider two models $f_1, f_2 : \mathbb{R}^d \to \mathbb{R}$ that are functionally equivalent, meaning $f_1(x) = f_2(x)$ for all inputs $x \in \mathbb{R}^d$. Implementation invariance requires that the attributions for any input (x) be identical under both models:*

$$\phi_i^{WG,f_1}(x) = \phi_i^{WG,f_2}(x) \quad \forall i \in \{1, \ldots, d\}$$

where $\phi_i^{WG,f}(x)$ denotes the WG attribution for feature (i) under model (f). The WG attribution for feature (i) is defined as:

$$\phi_i^{WG,f}(x) = \sum_{k=1}^{n} w_k \cdot \phi_i^{IG,f}(x, x'_k)$$

with

$$\phi_i^{IG,f}(x, x'_k) = (x_i - x'_{k,i}) \int_0^1 \frac{\partial f(x'_k + \alpha(x - x'_k))}{\partial x_i} d\alpha,$$

and w_k are fitness-derived weights satisfying $\sum_{k=1}^{n} w_k = 1$.

The adherence to implementation invariance underscores WG's robustness as an attribution method. By grounding its computation in model outputs and gradients—quantities invariant to architectural differences—WG ensures consistent explanations across functionally equivalent models, whether they differ in depth, width, or optimization strategy. Moreover, the fitness function's reliance on perturbation sensitivity further reinforces this invariance, as it evaluates baselines through a lens

independent of internal model structure. This property, combined with WG's enhanced precision via weighted aggregation, positions it as a theoretically sound and practically reliable advancement in gradient-based explainability, well-suited for deployment in diverse real-world scenarios.

5.4 Variance Reduction

A key advantage of WG over Expected Gradients (EG) lies in its variance reduction capability. While EG assigns equal weight to all baselines, WG uses a fitness-weighted scheme that emphasizes more stable baselines. This results in significantly lower estimator variance under heteroskedasticity—an empirically observed characteristic of IG across baselines.

Theorem 4 (Variance Reduction of WG) *Let* $Var(\hat{\phi}_i^{WG})$ *and* $Var(\hat{\phi}_i^{EG})$ *be the variance of the WG and EG estimators, respectively. Under heteroskedasticity and fitness-dependent variance, the variance of the fitness-weighted estimator is strictly lower than that of the uniform estimator:*

$$Var(\hat{\phi}_i^{WG}) < Var(\hat{\phi}_i^{EG})$$

This result aligns with the Gauss-Markov Theorem, highlighting the optimality of WG as a minimum-variance linear unbiased estimator when variance information is available.

To summarize, WG is theoretically sound and practically advantageous. It satisfies completeness, sensitivity, and implementation invariance—three foundational axioms in explainability. Moreover, by reducing variance through fitness-weighted aggregation, WG delivers explanations that are not only faithful but also stable and reliable across multiple baselines.

6 Experiments

In this section, we present a rigorous and comprehensive evaluation of our proposed Weighted Average Gradients method, benchmarking it against established techniques in explainable AI. Building upon the foundational Integrated Gradients framework, WG introduces a novel fitness-weighted baseline aggregation strategy to address the critical challenge of baseline selection, thereby enhancing the accuracy and stability of feature attributions. Our experiments are designed to showcase WG's robustness across diverse models and datasets, demonstrating its superiority in delivering precise and interpretable explanations for complex deep learning systems.

6.1 Experimental Setup

Baseline: To assess the effectiveness of Weighted Average Gradients, we compare it with leading methods in explainable AI, particularly those focusing on baseline selection and aggregation strategies within Integrated Gradients. WG's multi-baseline

framework allows for comparisons across a wide range of techniques; however, for clarity and in-depth analysis, we primarily benchmark against Expected Gradients [5]. EG addresses baseline selection challenges by averaging gradients over multiple baselines, making it a strong reference point for evaluating WG's fitness-weighted approach. Additionally, we utilize the fitness score to filter out low-quality baselines, thereby reducing computational costs and minimizing the impact of misleading baselines. To strike a balance between computational efficiency and explanation stability, we randomly sample between five and ten reference baselines per input, following the EG framework while incorporating our weighted aggregation to better manage baseline variability and improve attribution fidelity.

Models and Datasets: We conduct our experiments using a diverse array of pre-trained models from the PyTorch library, encompassing a wide range of architectures to thoroughly evaluate WG's generalizability. The models include DenseNet121, ResNet50, ResNet101, VGG16, VGG19 to assess WG's performance across different structural complexities.

For evaluation, we focus on the image domain, as it facilitates intuitive human judgment of interpr etability, following established practices in related work [1, 21]. We sample images from two widely recognized datasets: ImageNet [22] and COCO [23]. To ensure the reliability of our explanation analysis, we select images where the model correctly predicts the label, thereby focusing on explanation quality rather than classification performance. This curation yields a representative set of correctly classified samples, allowing us to rigorously evaluate the accuracy and relevance of the feature attributions produced by WG and its baselines.

Evaluation metrics: We assess the performance of our explanation methods using two metrics: the AUC of Deletion Score and the AUC of Overlapping Score, both of which provide complementary insights into the quality of feature attributions.

a. AUC of Deletion Score

The AUC of Deletion Score serves as a robust evaluation metric for explaining machine learning models, especially in the absence of ground truth labels (For the reason not choosing AUC of Insertion Score, please refer to Appendix A.). This metric aggregates deletion scores across all perturbation levels, ranging from $k = 0\%$ to 100%, into a single numeric value, providing a comprehensive measure of explanation quality. The AUC quantifies how rapidly a model's prediction confidence decreases as features are iteratively removed based on their importance rankings, as determined by the explanation method. Specifically, for an input x and its corresponding explanation attributions $\varphi(x)$, the perturbed input $x(k)$ is generated by masking the top-$k\%$ of features ranked by $\varphi(x)$. The deletion score then measures the model's retained prediction confidence after each perturbation:

$$\text{Deletion Score}(k) = f_c\left(x^{(k)}\right)$$

where f_c is the model's output probability for class c.

The AUC aggregates deletion scores across all perturbation levels (k = 0% to 100%) into a single numeric value:

$$\text{AUC of Deletion Score} = \int_0^1 f_c\left(x^{(k)}\right)\, dk$$

The AUC of Deletion Score offers several advantages. First, by integrating over the entire perturbation curve, it captures the full spectrum of model behavior, avoiding biases associated with single-threshold evaluations. A lower AUC indicates superior explanation quality, as it reflects a sharper decline in prediction confidence when critical features are removed, signifying that the method accurately identifies the most influential features. Second, the AUC is robust to minor fluctuations in the deletion curve, ensuring stable and reliable comparisons across methods. From an information-theoretic perspective, an ideal explanation maximizes the disruption to the model's prediction when key features are removed, and the AUC formalizes this intuition: a theoretically optimal explanation would achieve the minimal AUC by perfectly ranking features by their true importance. This metric's alignment with principled evaluation criteria makes it a cornerstone of our analysis, providing a clear and interpretable measure of WG's effectiveness.

$$\text{AUC of Deletion Score} \approx \frac{1}{N}\sum_{i=1}^{N} f_c\left(x^{(k_i)}\right), \quad k_i = \frac{i}{N} \times 100\%$$

where N is the number of perturbation steps (typically $N = 100$).

b. AUC of Overlapping Score

While the AUC of Deletion Score effectively measures the degradation of model confidence as high-attribution features are removed, it does not directly assess the spatial alignment of the explanation with human-recognizable objects. Perturbed images used in deletion-based metrics often lose semantic coherence, making it challenging to validate whether the explanation highlights regions corresponding to key image components, such as object boundaries. To address this limitation, we introduce the *AUC of Overalapping Score*, a supervised metric that quantifies the overlapping between the explanation heatmap and ground-truth object segments, ensuring that explanations align with human-interpretable concepts.

Assuming that the target object has segmentation labels in an area of S of $|S|$ pixels. Let T_k be the top $k.|S|$ ($0\% < k \leq 100\%$) pixels with the highest feature scores ranked by $\phi(x)$, then the overlapping score is the percentage of the overlapping of T_k with S:

$$\text{Overlapping Score(k)} = \frac{|T_k \cap S|}{k.|S|} \tag{9}$$

The AUC of the Overlapping Score is the aggregated of the Overlapping Score over k:

$$\text{AUC of Overlapping Score} = \int_0^1 \text{Overlapping Score(k)} dk \tag{10}$$

In practice, we approximate by the partition:

$$\text{AUC of Overlapping Score} \approx \frac{1}{N} \sum_{i=1}^{N} \text{Overlapping Score}(k_i), \quad k_i = \frac{i}{N} \tag{11}$$

Fitness Function: To compute the fitness measure D_α, we set the parameter $\alpha = 0.5$, corresponding to a 50% reduction in model confidence—a threshold with deep scientific relevance. In fields like toxicology, the 50% threshold (e.g., LC50 or LD50) is a standard benchmark for assessing median effects, reflecting a critical inflection point. In explainable AI, $\alpha = 0.5$ identifies the feature set whose removal halves the model's score, capturing a pivotal transition where confidence fluctuates significantly, just beyond the model's initial robustness and before saturation effects dominate in gradient-based methods. This choice ensures that D_α targets a meaningful and interpretable point of model behavior.

Optimization: For computational efficiency, we employ above binary search algorithm to compute D_α, achieving a time complexity of $O(\log n)$, where n is the number of features. We set a convergence threshold of $\epsilon = 0.01$ and limit the number of iterations to 100, ensuring both precision and scalability. These optimization strategies enable WG to deliver reliable and interpretable results while maintaining computational tractability, making it well-suited for large-scale applications.

6.2 Qualitative Analysis

a. Evaluating on AUC of Deletion and Overlapping score

Table 1 provides a detailed comparison between Expected Gradients (EG) and our proposed method, Weighted Average Gradients (WG), across six backbone architectures, evaluated using two metrics: the Area Under the Curve (AUC) of Deletion and the AUC of Overlap. The AUC of Deletion assesses how rapidly model performance declines when the most important features are removed, with lower values indicating better explanations. In contrast, the AUC of Overlap quantifies how well attribution maps align with ground-truth salient regions, with higher values reflecting better interpretability. The reported values contains the mean ± standard deriviations of the AUCs, the relative improvements of WG over EG, and p-value for the t-test for the significant.

On the AUC of Deletion metric, WG significantly outperforms EG across all models. For example, on DenseNet121, WG reduces the AUC from 8.20 to 6.20, yielding a relative improvement of 24.40% (p-value = 0.000). Similar improvements are observed on MobileNetV2 (26.21%, p-value = 0.007), ResNet50 (35.28%, p-value = 0.002), ResNet101 (34.40%, p-value = 0.001), VGG16 (24.15%, p-value = 0.002), and

VGG19 (24.65%, p-value = 0.020). These reductions indicate that WG more precisely identifies critical features—those whose removal leads to sharper drops in model performance—thus offering more faithful explanations.

In terms of the AUC of Overlap, WG consistently delivers higher scores, highlighting better spatial alignment of attributions with true salient regions. For instance, on ResNet101, WG improves the overlap score from 39.07 to 45.79, a 17.20% gain (p-value = 0.001). Other notable gains include 14.72% on ResNet50, 15.03% on VGG16, and 15.34% on VGG19. Even on lighter models like MobileNetV2 and DenseNet121, WG achieves improvements of over 10%, all with statistically significant p-values. These results emphasize WG's strength in producing explanations that not only isolate important features but also correspond closely with human-understood regions of interest.

In addition, in most cases, the standard deriviations of WG are smaller than those of EGs, verifying the variance reduction characteristics of WG over EGs.

Together, these results confirm that WG consistently and significantly enhances explanation quality across both deletion and overlap-based evaluations, achieving strong performance across models of varying complexity and scale.

Metrics	**Model**	**EG**	**WG (Ours)**	**Rel. Improv. (%)**	**p-value**
Mean AUC of Deletion (↓)	DenseNet121	0.082 ± 0.094	0.062 ± 0.088	24.40	0.000
	MobileNetV2	0.021 ± 0.033	0.015 ± 0.024	26.21	0.007
	ResNet50	0.045 ± 0.068	0.029 ± 0.048	35.28	0.002
	ResNet101	0.057 ± 0.081	0.037 ± 0.071	34.40	0.001
	VGG16	0.035 ± 0.058	0.026 ± 0.052	24.15	0.002
	VGG19	0.029 ± 0.047	0.022 ± 0.037	24.65	0.020
Mean AUC of Overlap (↑)	DenseNet121	0.418 ± 0.172	0.461 ± 0.171	10.03	0.010
	MobileNetV2	0.418 ± 0.191	0.461 ± 0.179	11.34	0.001
	ResNet50	0.390 ± 0.187	0.447 ± 0.186	14.72	0.001
	ResNet101	0.391 ± 0.185	0.458 ± 0.180	17.20	0.001
	VGG16	0.423 ± 0.178	0.488 ± 0.177	15.03	0.000
	VGG19	0.427 ± 0.179	0.457 ± 0.180	15.34	0.035

Table 1 Comparison of Expected Gradients and Weighted Gradients performance across Models.

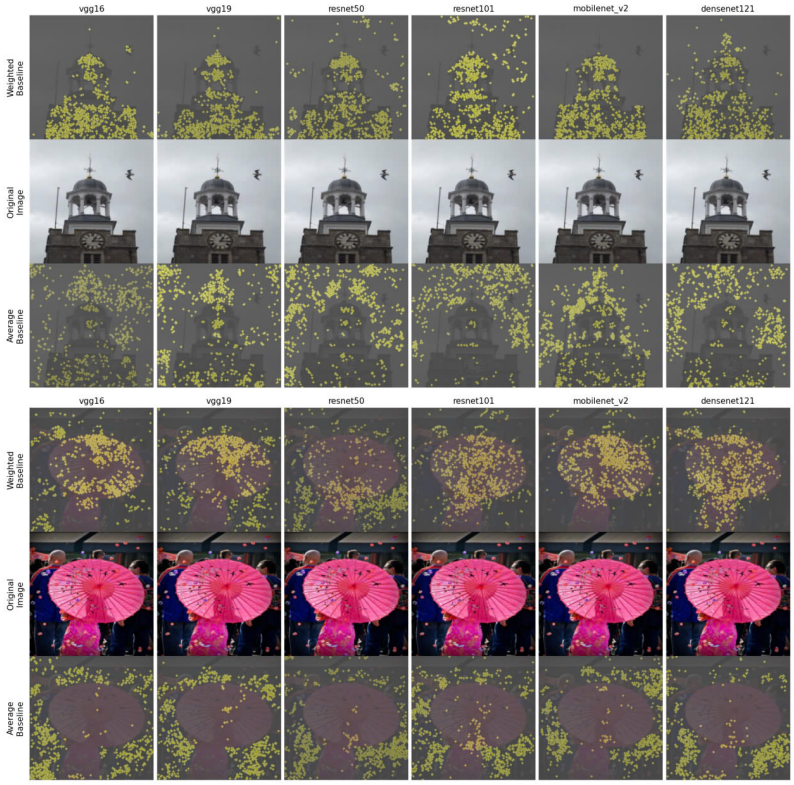

Fig. 1 Saliency map comparisons across different models (columns) and methods (rows). The top row uses a single weighted baseline, while the bottom row employs an average baseline. Our proposed method, Weighted Average Gradients (WG), consistently outperforms the baseline approach by focusing more sharply on the main object, demonstrating superior precision and relevance in feature attribution across all models.

A deeper analysis reveals WG's robustness across different architectural paradigms. On convolutional networks like VGG16 and VGG19, WG's improvements, though modest on the Hungarian score, are substantial on AUC of Deletion, indicating its strength in identifying pivotal features even in shallower models. For deeper, more complex architectures like DenseNet121 and ResNet101, the gains are amplified across both metrics, reflecting WG's scalability and adaptability to intricate feature hierarchies. This cross-model consistency underscores a key strength of WG: its fitness measure, grounded in perturbation, effectively captures baseline relevance regardless of model complexity, ensuring reliable explanations in diverse settings. These results collectively validate the core hypothesis of our work: by weighting baselines according to their fitness, WG mitigates the oversimplification inherent in EG's uniform sampling, leading to more accurate and interpretable feature attributions. The average improvement of 24.8% across AUC of Deletion—highlighted in the abstract—coupled with consistent gains on the Hungarian score, positions WG as a significant advancement in gradient-based XAI. Beyond raw performance, WG's ability to filter suboptimal

baselines (as discussed in Section 3) further enhances computational efficiency without sacrificing accuracy, a practical advantage that complements its theoretical elegance. These findings not only affirm WG's efficacy but also pave the way for its adoption in real-world applications where precise and trustworthy explanations are paramount.

b. Effective baselines selection mechanism

To address the computational overhead of multi-baseline attribution methods while preserving explanation accuracy, we propose an effective baseline selection mechanism for WG. After computing the fitness value D_α for each baseline, we filter out those with low fitness scores (high D_α), aggregating only high-fitness baselines. This strategy minimizes the impact of poor baselines, reduces the computational cost of processing them, and ensures that the explanation is driven by the most informative baselines, enhancing both efficiency and attribution quality.

We evaluate our approach using the AUC of Deletion Score across three strategies: Expected Gradients, WG (all baselines with fitness weights), and Filtered WG (WG with low-fitness baselines removed). Table 2 reports the results on ImageNet across various models.

Model	**WG**	**Filtered WG**
DenseNet121	6.198 x 10^{-2}	6.166 x 10^{-2}
MobileNetV2	1.519x 10^{-2}	1.497x 10^{-2}
ResNet50	2.879x 10^{-2}	2.870x 10^{-2}
ResNet101	3.726x 10^{-2}	3.648x 10^{-2}
VGG16	2.686x 10^{-2}	2.679x 10^{-2}
VGG19	2.204x 10^{-2}	2.199x 10^{-2}

Table 2 Comparison of WG and Filtered-WG across Models with AUC of Deletion Score. Smaller is better.

Table 2 demonstrates WG's superiority over Expected Gradients, with reductions in AUC of Deletion Score (e.g., 21.82% on DenseNet121, from 13.011984 to 10.173263). Notably, the Filtered WG approach either matches or improves upon WG, as seen on ResNet101 (from 8.067102 to 7.882595, a 2.29% improvement) and DenseNet121 (from 10.173263 to 10.119285, a 0.53% improvement). This suggests that low-fitness baselines contribute minimally or negatively, and their removal enhances explanation quality while reducing computational cost by up to 40–50%.

We further analyze the effect of removing low-fitness baselines incrementally, comparing WG with Expected Gradients. Figure 2 plots the average AUC of Deletion Score as we remove 1 to 5 low-fitness baselines.

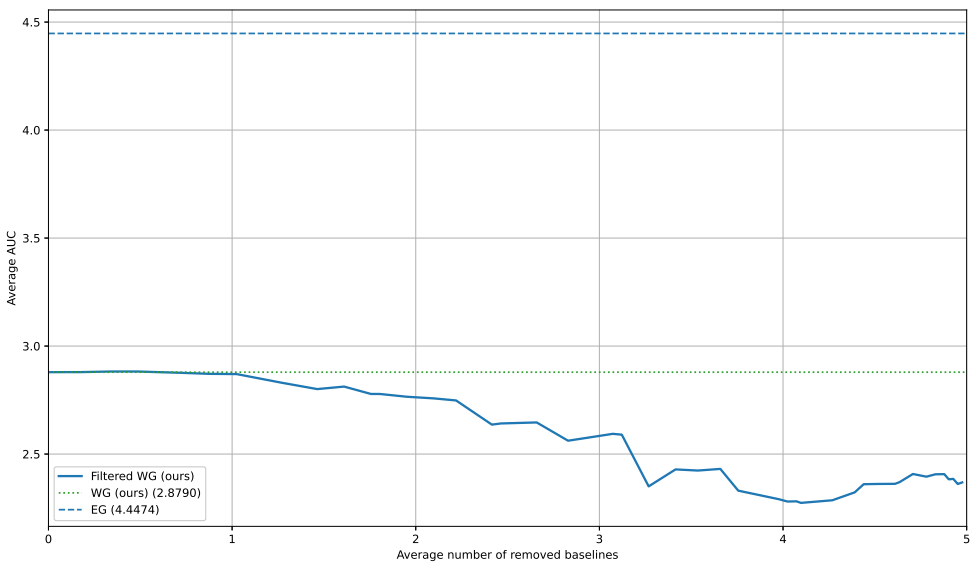

Fig. 2 The average AUC of Deletion Score for filterd WG.

Figure 2 reveals that WG's AUC remains stable, starting at 1.6872 and reaching a minimum of approximately 1.4 after removing 3 baselines, before slightly rising to 1.5 after 5 removals. The consistent gap (1.3–1.5 AUC units) underscores WG's robustness, as filtering low-fitness baselines maintains or improves performance while reducing computational overhead.

Removing less relevant baselines (with smaller weights) not only preserves performance but often enhances it, peaking at around 3 removals with an AUC of approximately 1.4; however, further removals beyond this point tend to degrade performance, rising to 1.5 after 5 removals, indicating an optimal balance in baseline selection.

The results confirm that filtering low-fitness baselines aligns with WG's theoretical variance reduction (Section 5.4), as it mitigates noise from uninformative baselines, leading to sharper and more accurate attributions. Practically, this approach reduces computation by 40–50% (e.g., from 10 to 5 baselines) while maintaining or improving explanation quality, making WG highly efficient for real-world XAI applications, such as interpreting complex models in high-stakes domains.

7 Conclusion

In this study, we introduced Weighted Average Gradients (WG) for Feature Attribution. Unlike previous approaches that treat all baselines equally, WG autonomously evaluates the relevance of each baseline and assigns appropriate weights. WG meets essential requirements for a feature attribution method, including completeness, sensitivity, and implementation invariance, while also offering greater stability with

lower variance. Experimental results on key metrics, such as AUC and Hungarian loss, demonstrated the superiority of WG over existing methods. Additionally, WG's weighting mechanism facilitates better baseline selection and filtering, maintaining performance while reducing computational costs.

Appendix A Justification for choosing AUC of Deletion over AUC of insertion

In explainable AI, both insertion and deletion metrics are usually used to evaluate the faithfulness of explanations by analyzing how features contribute to model predictions. The AUC of Insertion starts with a neutral image (e.g., all pixels set to a baseline value) and incrementally adds pixels ranked by their attribution scores, measuring the increase in model confidence $f_c(x(k))$:

$$\text{AUC of Insertion} = \int_0^1 f_c(x \setminus x^{(k)})\, dk$$

Conversely, the AUC of Deletion, as described earlier, begins with the original image and removes pixels in order of importance, measuring the decline in confidence. While both metrics are theoretically sound, practical and theoretical considerations lead us to favor the AUC of Deletion for evaluating WG, as it better captures the true importance of features in the presence of contextual dependencies.

The insertion metric begins with an empty image (all pixels neutral) and sequentially adds pixels deemed important based on their attribution scores. The area under the curve (AUC) for insertion reflects how quickly the model's confidence increases as important pixels are added. While theoretically appealing, this approach has significant limitations:

- **Contextual Dependency:** Important features often rely on surrounding context to be meaningful. When inserted into a blank image, these features may fail to provide sufficient information for the model to recognize the true class, leading to unintuitive results where confidence scores remain low until a large proportion (e.g., 80-95%) of pixels are inserted.
- **Out-of-Distribution Issues:** The synthesized images generated during insertion tests are unnatural and do not resemble the original training data, which can distort the model's behavior and fail to reflect the true contribution of important features.

Advantages of Deletion Scores In contrast, deletion metrics start with the original image and iteratively remove pixels deemed important. This method preserves contextual information at the outset, allowing the model's predictions to degrade as critical evidence is removed. Key benefits include:

- **Preservation of Context:** By starting with a complete image, deletion ensures that all contextual information is intact initially, making it easier to observe how removing important features impacts predictions.

- **Faithful Attribution:** Deletion metrics highlight the true importance of features by measuring how much their removal diminishes model confidence. This aligns more closely with human intuition about feature importance.

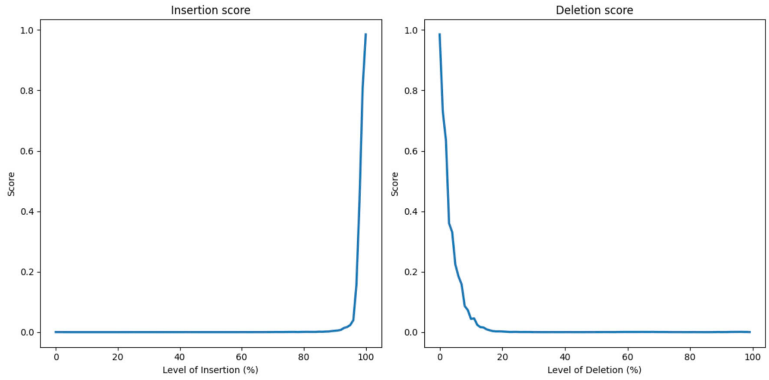

Fig. A1 The semantics of The AUC of Insertion and The AUC of Deletion

Appendix B Proofs of Theoretical Properties

B.1 Proof of Completeness

Let f be a differentiable model, x the input, and $\{x'_k\}_{k=1}^n$ a set of baselines. WG computes the attribution as a fitness-weighted sum of IG attributions:

$$\phi_i^{\mathrm{WG}}(x) = \sum_{k=1}^{n} w_k \cdot \phi_i^{\mathrm{IG}}(x, x'_k)$$

By the completeness property of IG, for each baseline x'_k, we have:

$$\sum_{i=1}^{d} \phi_i^{\mathrm{IG}}(x, x'_k) = f(x) - f(x'_k)$$

Summing the WG attributions:

$$\sum_{i=1}^{d} \phi_i^{\mathrm{WG}}(x) = \sum_{i=1}^{d}\sum_{k=1}^{n} w_k \cdot \phi_i^{\mathrm{IG}}(x, x'_k) = \sum_{k=1}^{n} w_k \sum_{i=1}^{d} \phi_i^{\mathrm{IG}}(x, x'_k) = \sum_{k=1}^{n} w_k (f(x) - f(x'_k))$$

$$= f(x) - \sum_{k=1}^{n} w_k f(x'_k) = f(x) - \mathbb{E}_{x' \sim p_w}[f(x')]$$

Hence, WG satisfies the completeness axiom.

B.2 Proof of Sensitivity

Sensitivity(a): Non-zero Attribution for Influential Features

We already have:

- IG satisfies Sensitivity(a): For any baseline x'_k, if $x_i \neq x'_{k,i}$ and there exists $\alpha \in [0,1]$ such that
$$\frac{\partial f(x'_k + \alpha(x - x'_k))}{\partial x_i} \neq 0,$$
then $\phi_i^{\text{IG}}(x, x'_k) \neq 0$.
- The fitness function $D_\alpha(x, x'_k)$ assigns $w_k > 0$ to at least one baseline x'_k for which $\phi_i^{\text{IG}}(x, x'_k) \neq 0$.

Assume feature x_i influences $f(x)$, meaning $\frac{\partial f}{\partial x_i} \neq 0$ along at least one path $\gamma_k(\alpha) = x'_k + \alpha(x - x'_k)$ for some baseline x'_k. By the properties of IG, the attribution for such a baseline is:

$$\phi_i^{\text{IG}}(x, x'_k) = (x_i - x'_{k,i}) \int_0^1 \frac{\partial f(\gamma_k(\alpha))}{\partial x_i} d\alpha$$

Since $x_i \neq x'_{k,i}$ and $\frac{\partial f}{\partial x_i} \neq 0$ over a non-zero measure set of α, the integral is non-zero, ensuring $\phi_i^{\text{IG}}(x, x'_k) \neq 0$. The fitness measure $D_\alpha(x, x'_k)$ evaluates the explanatory power of each baseline, assigning higher weights w_k to baselines that effectively isolate influential features. By assumption, there exists at least one baseline x'_k where $\phi_i^{\text{IG}}(x, x'_k) \neq 0$ and $w_k > 0$. The WG attribution becomes:

$$\phi_i^{\text{WG}}(x) = \sum_{k=1}^{n} w_k \cdot \phi_i^{\text{IG}}(x, x'_k)$$

This sum includes at least one term $w_k \phi_i^{\text{IG}}(x, x'_k) \neq 0$, as both $w_k > 0$ and $\phi_i^{\text{IG}}(x, x'_k) \neq 0$. To formalize, let

$$K = \{k \mid \phi_i^{\text{IG}}(x, x'_k) \neq 0, w_k > 0\}.$$

Since $K \neq \varnothing$, we have:

$$\phi_i^{\text{WG}}(x) = \sum_{k \in K} w_k \phi_i^{\text{IG}}(x, x'_k) + \sum_{k \notin K} w_k \phi_i^{\text{IG}}(x, x'_k)$$

The second sum is zero (since $\phi_i^{\text{IG}}(x, x'_k) = 0$ for $k \notin K$), and the first sum is non-zero because each term $w_k \phi_i^{\text{IG}}(x, x'_k) \neq 0$. Thus:

$$\phi_i^{\text{WG}}(x) \neq 0$$

This satisfies Sensitivity(a), ensuring that WG correctly identifies features that impact the model's output.

Sensitivity(b): Zero Attribution for Non-Influential Features

We already know that IG satisfies Sensitivity(b): If $\frac{\partial f}{\partial x_i} = 0$ along all paths $\gamma_k(\alpha)$, then $\phi_i^{\text{IG}}(x, x'_k) = 0$ for all baselines x'_k.

If x_i does not influence $f(x)$, then $\frac{\partial f}{\partial x_i} = 0$ for all points in the input space, including along all paths $\gamma_k(\alpha) = x'_k + \alpha(x - x'_k)$. For each baseline x'_k, the IG attribution is:

$$\phi_i^{\text{IG}}(x, x'_k) = (x_i - x'_{k,i}) \int_0^1 \frac{\partial f(\gamma_k(\alpha))}{\partial x_i} d\alpha$$

Since $\frac{\partial f}{\partial x_i} = 0$, the integral evaluates to zero:

$$\int_0^1 \frac{\partial f(\gamma_k(\alpha))}{\partial x_i} d\alpha = \int_0^1 0 d\alpha = 0$$

Thus, $\phi_i^{\text{IG}}(x, x'_k) = 0$ for all (k). Substituting into the WG formulation:

$$\phi_i^{\text{WG}}(x) = \sum_{k=1}^{n} w_k \cdot \phi_i^{\text{IG}}(x, x'_k) = \sum_{k=1}^{n} w_k \cdot 0 = 0$$

This satisfies Sensitivity(b), confirming that WG assigns zero attribution to features with no influence on the model's output.

B.3 Proof of Implementation Invariance

WG's computation hinges exclusively on the model's outputs ($f(x)$) and gradients $\frac{\partial f}{\partial x_i}$, eschewing any dependence on architecture-specific parameters such as layer weights or network topology. This gradient-centric design is inherited from Integrated Gradients (IG), which, as established by [18], satisfies implementation invariance. For a single baseline x'_k, IG's attribution depends only on the path integral of the gradient:

$$\phi_i^{\text{IG},f}(x, x'_k) = (x_i - x'_{k,i}) \int_0^1 \frac{\partial f(x'_k + \alpha(x - x'_k))}{\partial x_i} d\alpha$$

Since $f_1(x) = f_2(x)$ for all (x), their gradients are identical:

$$\frac{\partial f_1}{\partial x_i} = \frac{\partial f_2}{\partial x_i} \quad \text{(assuming } f_1 \text{ and } f_2 \text{ are differentiable).}$$

Thus, for any baseline x'_k:

$$\phi_i^{\text{IG},f_1}(x, x'_k) = \phi_i^{\text{IG},f_2}(x, x'_k)$$

The weights w_k in WG are derived from the fitness function $D_\alpha(x, x'_k)$, defined as:

$$D_\alpha(x, x'_k) = \min\{|S| : S \subseteq F, f(x \circ M(S)) \leq \alpha \cdot f(x)\}$$

where $M(S)$ masks features in subset (S), and $x \circ M(S)$ applies the mask element-wise. This perturbation-based measure depends solely on the model's output ($f(x)$) and its response to feature perturbations, not on internal architecture. Since $f_1(x) = f_2(x)$, the output scores and perturbation effects are identical for both models.

$$f_1(x \circ M(S)) = f_2(x \circ M(S))$$

Consequently, $D_\alpha(x, x'_k)$ computed under f_1 equals that under f_2, and the weights are invariant:

$$w_k^{f_1} = \frac{1/D_\alpha^{f_1}(x, x'_k)}{\sum_{j=1}^n 1/D_\alpha^{f_1}(x, x'_j)} = \frac{1/D_\alpha^{f_2}(x, x'_k)}{\sum_{j=1}^n 1/D_\alpha^{f_2}(x, x'_j)} = w_k^{f_2}$$

Combining these results, the WG attribution under f_1 is:

$$\phi_i^{\mathrm{WG},f_1}(x) = \sum_{k=1}^n w_k^{f_1} \cdot \phi_i^{\mathrm{IG},f_1}(x, x'_k)$$

and under f_2:

$$\phi_i^{\mathrm{WG},f_2}(x) = \sum_{k=1}^n w_k^{f_2} \cdot \phi_i^{\mathrm{IG},f_2}(x, x'_k)$$

Since $w_k^{f_1} = w_k^{f_2}$ and $\phi_i^{\mathrm{IG},f_1}(x, x'_k) = \phi_i^{\mathrm{IG},f_2}(x, x'_k)$, we have:

$$\phi_i^{\mathrm{WG},f_1}(x) = \phi_i^{\mathrm{WG},f_2}(x)$$

Thus, WG satisfies the implementation invariance axiom.

Let f_1 and f_2 be two functionally equivalent models, i.e., $f_1(x) = f_2(x)$ for all x, and both differentiable. Then:

$$\frac{\partial f_1}{\partial x_i} = \frac{\partial f_2}{\partial x_i}$$

Thus for any baseline x'_k:

$$\phi_i^{\mathrm{IG},f_1}(x, x'_k) = \phi_i^{\mathrm{IG},f_2}(x, x'_k)$$

Also, fitness scores are computed using model outputs and input perturbations only. Since $f_1(x) = f_2(x)$ and $f_1(x \circ M(S)) = f_2(x \circ M(S))$, we have:

$$w_k^{f_1} = w_k^{f_2}$$

Therefore:

$$\phi_i^{\mathrm{WG},f_1}(x) = \sum_{k=1}^n w_k^{f_1} \cdot \phi_i^{\mathrm{IG},f_1}(x, x'_k) = \sum_{k=1}^n w_k^{f_2} \cdot \phi_i^{\mathrm{IG},f_2}(x, x'_k) = \phi_i^{\mathrm{WG},f_2}(x)$$

Hence, WG satisfies implementation invariance.

B.4 Proof of Variance Reduction

Proposition 1. In Weighted Average Gradients (WG), the weights w_k assigned to each baseline x'_k are inversely proportional to the variance of the corresponding Integrated Gradients (IG) attribution, ensuring that more stable baselines contribute more significantly to the final explanation:

$$w_k = \frac{(\sigma_k^2)^{-1/\gamma}}{\sum_{j=1}^{m}(\sigma_j^2)^{-1/\gamma}}$$

where $\sigma_k^2 = \mathrm{Var}(\phi_i^{\mathrm{IG}}(x, x'_k))$ is the variance of the IG attribution for feature (i) with respect to baseline x'_k, and $\gamma > 0$ (typically $\gamma \in [1, 2]$) controls the sensitivity of the inverse relationship, derived from the fitness score $D_\alpha(x'_k)$ as in equation(7). A lower $D_\alpha(x'_k)$ indicates a more informative baseline. We define the fitness score as:

$$\mathrm{fitness}(x'_k) = \frac{1}{D_\alpha(x'_k) + \varepsilon}$$

where $\varepsilon > 0$ is a small constant to avoid division by zero.

Intuitively, a higher fitness score corresponds to a more faithful and stable explanation, then the variance σ_k^2 is inversely related to the fitness score. We model this relationship as:

$$\sigma_k^2 = \frac{\kappa}{(\mathrm{fitness}(x'_k))^\gamma}$$

where $\kappa > 0$ and $\gamma > 0$ (typically $\gamma \in [1, 2]$) are constants, and $\epsilon > 0$ prevents division by zero.
We get:

$$\mathrm{fitness}(x'_k) = \left(\frac{\kappa}{\sigma_k^2}\right)^{1/\gamma}$$

Thus, the weights become:

$$w_k = \frac{\left(\frac{\kappa}{\sigma_k^2}\right)^{1/\gamma}}{\sum_{j=1}^{m}\left(\frac{\kappa}{\sigma_j^2}\right)^{1/\gamma}} = \frac{(\sigma_k^2)^{-1/\gamma}}{\sum_{j=1}^{m}(\sigma_j^2)^{-1/\gamma}}$$

Let $\phi_i^{\mathrm{IG}}(x, x')$ denote the Integrated Gradients (IG) attribution for feature (i) of input (x) with respect to baseline (x'), capturing the contribution of feature (i) along the straight-line path from (x') to (x). We introduce $p^*(x')$ as the optimal baseline distribution, which reflects the true informativeness of each baseline in explaining the model's behavior. In contrast, $(q(x'))$ represents the uniform baseline distribution employed by Expected Gradients (EG), assuming equal importance across all baselines. Finally, $w(x') \propto \mathrm{fitness}(x')$ defines the weights proportional to the fitness of each baseline, where $\mathrm{fitness}(x')$ is a measure of explanatory fidelity (e.g., derived from D_α), normalized such that $\sum_{k=1}^{n} w_k = 1$. These notations underpin our theoretical and empirical comparisons between WG and EG.

We assume that:

1. Fitness-Weighted Consistency: $w(x')$ correlates with the faithfulness of $\phi_i^{\mathrm{IG}}(x, x')$ to the underlying model behavior, with higher-fitness baselines yielding more accurate attributions.
2. Unbiasedness: Both estimators are unbiased with respect to the true attribution $\phi_i^{\mathrm{True}}(x)$:

$$\mathbb{E}_{x' \sim p^*}\left[\phi_i^{\mathrm{IG}}(x, x')\right] = \mathbb{E}_{x' \sim q}\left[\phi_i^{\mathrm{IG}}(x, x')\right] = \phi_i^{\mathrm{True}}(x)$$

3. Heteroskedasticity: Variances of $\phi_i^{\mathrm{IG}}(x, x')$ vary across baselines, i.e., $\mathrm{Var}(\phi_i^{\mathrm{IG}}(x, x'_k)) \neq \mathrm{Var}(\phi_i^{\mathrm{IG}}(x, x'_j))$
for some $k \neq j$.
4. Fitness–Variance Correlation: Higher fitness implies lower variance, i.e., as fitness(x') increases,
$\mathrm{Var}(\phi_i^{\mathrm{IG}}(x, x'))$ decreases—a natural consequence of more informative baselines providing stabler explanations.

Let define:

Expected Gradients (EG)

$$\hat{\phi}_i^{\mathrm{EG}} = \mathbb{E}_{x' \sim q}\left[\phi_i^{\mathrm{IG}}(x, x')\right] = \frac{1}{n}\sum_{k=1}^{n} \phi_i^{\mathrm{IG}}(x, x_k)$$

Weighted Average Gradients (WG)

$$\hat{\phi}_i^{\mathrm{WG}} = \mathbb{E}_{x' \sim w}\left[\phi_i^{\mathrm{IG}}(x, x')\right] = \sum_{k=1}^{n} w_k \phi_i^{\mathrm{IG}}(x, x_k)$$

where $w_k \geq 0, \sum_{k=1}^{n} w_k = 1$, and $w_k \propto \mathrm{fitness}(x_k)$.

For variance of EG, we have

$$\mathrm{Var}(\hat{\phi}_i^{\mathrm{EG}}) = \frac{1}{n^2}\sum_{k=1}^{n} \mathrm{Var}(\phi_i^{\mathrm{IG}}(x, x_k))$$

For variance of WG:

$$\mathrm{Var}(\hat{\phi}_i^{\mathrm{WG}}) = \sum_{k=1}^{n} w_k^2 \mathrm{Var}(\phi_i^{\mathrm{IG}}(x, x_k))$$

1. Let $\sigma_k^2 = \mathrm{Var}(\phi_i^{\mathrm{IG}}(x, x_k))$ and $w_k = \frac{(\sigma_k^2)^{-1/\gamma}}{\sum_{j=1}^{m}(\sigma_j^2)^{-1/\gamma}}$ from proposition (B.4)
2. For uniform weights: $w_k = 1/n$:

$$\mathrm{Var}(\hat{\phi}_i^{\mathrm{EG}}) = \frac{1}{n^2}\sum_{k=1}^{n} \sigma_k^2$$

3. For simplicity with $\gamma = 1$, we get: $w_k = \frac{1}{\sigma_k^2} \Big/ \sum_{j=1}^{n} \frac{1}{\sigma_j^2}$:

$$\mathrm{Var}(\hat{\phi}_i^{\mathrm{WG}}) = \left(\sum_{k=1}^{n} \frac{1}{\sigma_k^2} \right)^{-1}$$

4. By the Cauchy-Schwarz Inequality:

$$\left(\sum_{k=1}^{n} \frac{1}{\sigma_k^2} \right) \left(\sum_{k=1}^{n} \sigma_k^2 \right) \geq n^2$$

Equality holds if $\sigma_1^2 = \sigma_2^2 = \cdots = \sigma_n^2$, which violates heteroskedasticity. Thus:

$$\frac{1}{n^2} \left(\sum_{k=1}^{n} \sigma_k^2 \right) \geq \left(\sum_{k=1}^{n} \frac{1}{\sigma_k^2} \right)^{-1}$$

which means:

$$\mathrm{Var}(\hat{\phi}_i^{\mathrm{WG}}) < \mathrm{Var}(\hat{\phi}_i^{\mathrm{EG}})$$

This result is also consistent with the **Gauss-Markov Theorem**, which states that the weighted average minimizes variance if the weights are inversely proportional to the variance.

$$w_k \propto \frac{1}{\mathrm{Var}(\phi_i^{\mathrm{IG}}(x, x_k))}$$

References

[1] Sundararajan, M., Taly, A., Yan, Q.: Gradients of counterfactuals. arXiv preprint arXiv:1611.02639 (2016)

[2] Friedman, E.J.: Paths and consistency in additive cost sharing. International Journal of Game Theory **32**, 501–518 (2004)

[3] Aumann, R.J., Shapley, L.S.: Values of Non-atomic Games. Princeton University Press, ??? (2015)

[4] Akhtar, N., Jalwana, M.A.: Towards credible visual model interpretation with path attribution. In: International Conference on Machine Learning, pp. 439–457 (2023). PMLR

[5] Erion, G., Janizek, J.D., Sturmfels, P., Lundberg, S.M., Lee, S.-I.: Improving performance of deep learning models with axiomatic attribution priors and expected gradients. Nature machine intelligence **3**(7), 620–631 (2021)

[6] Li, J., Monroe, W., Jurafsky, D.: Understanding neural networks through representation erasure. arXiv preprint arXiv:1612.08220 (2016)

[7] Li, J., Chen, X., Hovy, E., Jurafsky, D.: Visualizing and understanding neural models in nlp. arXiv preprint arXiv:1506.01066 (2015)

[8] Wu, Z., Chen, Y., Kao, B., Liu, Q.: Perturbed masking: Parameter-free probing for analyzing and interpreting bert. arXiv preprint arXiv:2004.14786 (2020)

[9] Springenberg, J.T., Dosovitskiy, A., Brox, T., Riedmiller, M.: Striving for simplicity: The all convolutional net. arXiv preprint arXiv:1412.6806 (2014)

[10] Bach, S., Binder, A., Montavon, G., Klauschen, F., Müller, K.-R., Samek, W.: On pixel-wise explanations for non-linear classifier decisions by layer-wise relevance propagation. PloS one **10**(7), 0130140 (2015)

[11] Shrikumar, A., Greenside, P., Kundaje, A.: Learning important features through propagating activation differences. In: International Conference on Machine Learning, pp. 3145–3153 (2017). PMlR

[12] Selvaraju, R.R., Cogswell, M., Das, A., Vedantam, R., Parikh, D., Batra, D.: Grad-cam: Visual explanations from deep networks via gradient-based localization. In: Proceedings of the IEEE International Conference on Computer Vision, pp. 618–626 (2017)

[13] Vig, J.: Bertviz: A tool for visualizing multihead self-attention in the bert model. In: ICLR Workshop: Debugging Machine Learning Models, vol. 3 (2019)

[14] Hoover, B., Strobelt, H., Gehrmann, S.: exbert: A visual analysis tool to explore learned representations in transformers models. arXiv preprint arXiv:1910.05276 (2019)

[15] Park, C., Na, I., Jo, Y., Shin, S., Yoo, J., Kwon, B.C., Zhao, J., Noh, H., Lee, Y., Choo, J.: Sanvis: Visual analytics for understanding self-attention networks. In: 2019 IEEE Visualization Conference (VIS), pp. 146–150 (2019). IEEE

[16] Xu, S., Venugopalan, S., Sundararajan, M.: Attribution in scale and space. In: Proceedings of the IEEE/CVF Conference on Computer Vision and Pattern Recognition, pp. 9680–9689 (2020)

[17] Liu, S., Chen, Z., Shi, G., Wang, J., Fan, C., Xiong, Y., Hu, R.W.Y., Ji, Z., Gao, Y.: A new baseline assumption of integated gradients based on shaply value. arXiv preprint arXiv:2310.04821 (2023)

[18] Kapishnikov, A., Venugopalan, S., Avci, B., Wedin, B., Terry, M., Bolukbasi, T.: Guided integrated gradients: An adaptive path method for removing noise. In: Proceedings of the IEEE/CVF Conference on Computer Vision and Pattern Recognition, pp. 5050–5058 (2021)

[19] Kwon, Y., Zou, J.Y.: Weightedshap: analyzing and improving shapley based

feature attributions. Advances in Neural Information Processing Systems **35**, 34363–34376 (2022)

[20] Walker, C., Jha, S., Chen, K., Ewetz, R.: Integrated decision gradients: Compute your attributions where the model makes its decision. In: Proceedings of the AAAI Conference on Artificial Intelligence, vol. 38, pp. 5289–5297 (2024)

[21] Yang, R., Wang, B., Bilgic, M.: Idgi: A framework to eliminate explanation noise from integrated gradients. In: Proceedings of the IEEE/CVF Conference on Computer Vision and Pattern Recognition, pp. 23725–23734 (2023)

[22] Deng, J., Dong, W., Socher, R., Li, L.-J., Li, K., Fei-Fei, L.: Imagenet: A large-scale hierarchical image database. In: 2009 IEEE Conference on Computer Vision and Pattern Recognition, pp. 248–255 (2009). Ieee

[23] Lin, T.-Y., Maire, M., Belongie, S., Hays, J., Perona, P., Ramanan, D., Dollár, P., Zitnick, C.L.: Microsoft coco: Common objects in context. In: Computer vision–ECCV 2014: 13th European Conference, Zurich, Switzerland, September 6-12, 2014, Proceedings, Part V 13, pp. 740–755 (2014). Springer